INFECTION AND IMMUNITY, July 2003, p. 4067–4078 Vol. 71, No. 7
0019-9567/03/$08.00+0 DOI: 10.1128/IAI.71.7.4067–4078.2003

Soluble Extracts from *Helicobacter pylori* Induce Dome Formation in Polarized Intestinal Epithelial Monolayers in a Laminin-Dependent Manner

A. M. Terrés,[1]* H. J. Windle,[1] E. Ardini,[2] and D. P. Kelleher[1]

Department of Clinical Medicine and Dublin Molecular Medicine Centre, Trinity College, Dublin, Ireland,[1] *and Division of Experimental Oncology, Istituto Nazionale Tumori, Milan, Italy*[2]

Received 29 October 2002/Returned for modification 24 December 2002/Accepted 22 April 2003

Helicobacter pylori **colonizes the stomach at the interface between the mucus layer and the apical pole of gastric epithelial cells. A number of secreted and shed products from the bacteria, such as proteins and lipopolysaccharide, are likely to have a role in the pathogenesis at the epithelial level. To determine the physiological response of transporting polarized epithelia to released soluble factors from the bacterium, we used the T84 cell line. Monolayers of T84 cells were exposed to soluble extracts from *H. pylori*. The extracts induced rapid "dome" formation as well as an immediate decrease in transepithelial electrical resistance. Domes are fluid-filled blister-like structures unique to polarized epithelia. Their formation has been linked to sodium-transporting events as well as to diminished adherence of the cells to the substrate. *H. pylori*-induced dome formation in T84 monolayers was exacerbated by amiloride and inhibited by ouabain. Furthermore, it was associated with changes in the expression of the laminin binding α6β4 integrin and the 67-kDa laminin receptor. Domes formed primarily on laminin-coated filters, rather than on fibronectin or collagen matrices, and their formation was inhibited by preincubating the bacterial extract with soluble laminin. This effect was specific to *H. pylori* and independent of the urease, vacA, cagA, and Lewis phenotype of the strains. These data indicate that released elements from *H. pylori* can alter the physiological balance and integrity of the epithelium in the absence of an underlying immune response.**

The gastrointestinal epithelium represents the first cellular barrier against intraluminal insults. In the stomach, the interface between the epithelial cells and the gastric mucus represents the ecological niche for the gram-negative bacterium *Helicobacter pylori*. The intimate association between the microorganism and the epithelium initiates a pathological response at the host epithelial surface which subsequently results in a specific local immune response (reviewed in reference 6). The direct effects in epithelial cells upon stimulation with *H. pylori* have been widely studied in vitro, and effects such as loss of epithelial barrier function (42, 55), cytoskeletal rearrangements (2), apoptosis (14), and induction of nuclear factor kappa B (39), interleukin 8, and cyclooxygenase-2 (22) have been reported. Upon onset of the infection, the subsequent inflammatory response, in particular to $CagA^+$ strains, also has an important effect in the epithelium, due to neutrophil transepithelial migration and associated releases of reactive oxygen intermediaries (41, 49).

The loss of epithelial homeostasis and integrity are likely to be the first in the cascade of events that leads to *H. pylori*-associated gastrointestinal pathogenesis. The enterocytes perform the barrier function by maintaining their polarity and tightly associating with each other through lateral adherents and tight junctions (35, 59). These cells also maintain a stable connection to basement membranes through adhesive interactions between the cells and extracellular matrix proteins (51), and the principal agent mediating the integration of the cytoskeleton and extracellular matrix is the integrin heterodimer α6β4 (16, 51).

The human intestinal epithelial cell line T84 differentiates in vitro into polarized monolayers with functional tight junctions which maintain an ion-transporting phenotype (28), representing a good in vitro model for the study of the physiological response to the gastrointestinal pathogen *H. pylori.*

It has been previously shown that sonicates and bacterial extracts from *H. pylori* can alter the paracellular barrier function (55), and Papini et al. (42) have shown that the bacterial vacuolating toxin can selectively increase the permeability of this cell line. These data indicate that *H. pylori* epithelial pathogenesis may be mediated not only by direct interaction with the organism, but also by released bacterial elements such as lipopolysaccharide (LPS) or secreted proteins. Since alterations of the epithelial physiology could contribute to the onset of *H. pylori*-associated disease, we aimed to study the physiological response of intestinal epithelial cells to soluble factors readily shed or secreted by the bacterium.

Although the understanding of how epithelial cells regulate tight junction-mediated permeability is still incomplete, the process of epithelial homeostasis control has been clarified (24). The lining of the intestine maintains cell volume and hydration as a result of ion transport processes involving a well-balanced control of Cl^- and Na^+ secretion and absorption (24). These cells have a polarized phenotype that facilitates a differential expression of ionic channels, pumps, and transporters in the apical or basolateral membrane domains (46). This is the case for the Na^+/K^+ ATPase, expressed basolaterally, or the Na^+/H^+ electrogenic epithelial sodium channel (ENaC), expressed only apically in colonic and small intestine epithelial cells (24). Important human diseases, such

* Corresponding author. Mailing address: Department of Clinical Medicine, Trinity Centre for Health Sciences, St. James Hospital, Dublin 8, Ireland. Phone: (353)-1-6082115. Fax: (353)-1-4542043. E-mail: amterres@tcd.ie.

as cystic fibrosis or secretory diarrhea, result when regulated ionic transport malfunctions (4).

A variety of epithelial cell lines that retain their transepithelial transport properties are able to form "domes" in vitro. Domes are localized blister-like areas of fluid accumulation between the cultured monolayer and the impermeable substrate (47) which have been interpreted as indicative of fluid transport (25), weak attachment to the substrate (52), and a sign of epithelial differentiation (26). Their presence demonstrates the maintenance of a differentiated polarized phenotype and the presence of functional tight junctional complexes. Some cell lines develop domes spontaneously upon reaching confluence, but others only develop them upon exposure to various stimuli, including cyclic AMP (cAMP) analogs, dimethyl sulfoxide (26), and retinoic acid (53).

In this study we show for the first time that apical stimulation of T84 monolayers with *H. pylori* extracts (HPE) induces the formation of domes. We set out to identify the molecular mechanism involved in the formation of these structures.

MATERIALS AND METHODS

Bacterial preparations. *H. pylori* reference strains NCTC 11637 and NCTC 11638 were obtained from the National Collection of Type Cultures (NCTC; Colindale, United Kingdom). The clinical isolates MI300, MI270, MI299, and MI215, used in comparative studies, have been previously characterized in terms of their Lewis x, Lewis y, vacA, and cagA phenotypes and association with disease (33). The following parental wild-type strains and isogenic mutants were also used: 60190 (ATCC 49503), 60190 *vacA*::*km* (20), 60190 *cagA*::*km* (43), 84183, 84183 *vacA*::*km* (constructed by R. Tomas, Nottingham University Hospital, as described in reference 10), N6, *N6 ureB*::*km* (15), and *N6 ureG*::*km* (13). Gram-negative bacteria, processed in the same fashion and used as controls, included *Escherichia coli* DH5α and the reference strain *Serratia marcescens* NCTC 11935 (NCTC) as well as a wild-type strain of *E. coli* isolated from a patient with a urinary tract infection. *H. pylori* was grown on blood agar plates for 72 h in a microaerobic and humidified atmosphere at 37°C. *E. coli* and *S. marcescens* cells were grown in blood agar plates at 37°C overnight. Bacteria were harvested into ice-cold tissue culture medium (see below) without fetal calf serum, unless indicated otherwise (1 ml/plate). Suspended bacteria were adjusted to an optical density at 600 nm of 2.9, placed on ice for 20 min, and then centrifuged (15,000 × *g*; 15 min; 4°C). The supernatant (HPE) was stored at −20°C until required. *H. pylori* NCTC 11638 was used for all experiments except where indicated.

Epithelial cell cultures. The epithelial cell line T84, obtained from the European Collection of Animal Cell Culture (ECACC; Salisbury, United Kingdom) was used in this study and cultured in Dulbecco's Ham's F12 medium (Sigma, Dorset, United Kingdom) as previously described (55). Only T84 cells between passages 60 and 75 were used in this study. The cell lines Caco-2 (human colonic, polarized), AGS (human gastric, nonpolarized), HCT116 (human colonic, nonpolarized), and MDCK (canine renal, polarized), all from ECACC, were also used for comparative purposes.

T84 cells were grown on semipermeable tissue culture inserts of uncoated polyethylene terephthalate (PET) plastic trace-etched membranes (Falcon; Beckton Dickinson, Oxford, United Kingdom), and cells were fed both apically and basally. For some experiments collagen I-, fibronectin-, or laminin-coated PET membrane cell culture inserts (area, 0.565 cm^2; pore diameter, 0.45 μm; Falcon; Beckton Dickinson) or uncoated transwell clear polyester membrane inserts (Costar, Cambridge, Mass.) were used. PET uncoated inserts were always used unless indicated otherwise.

Cell confluence was assessed by phase-contrast microscopy. Polarization and differentiation were monitored by measuring transepithelial electrical resistance (TER) as described previously (55). The resistance, monitored at 24-h intervals, increased progressively over 10 to 15 days when cells formed high-resistance polarized monolayers with stable TER values (~1,500 to 2,000 Ω/cm^2). At this stage the apical or basolateral cell culture medium, where appropriate, was substituted with HPE, incubated for various periods of time, and monitored or processed for immunofluorescence staining.

Antibodies and chemicals. The antibodies GoH3 rat anti-α6 integrin, (Serotec, Oxford, United Kingdom); rat anti-β4 integrin (Serotec); mouse anti-β1 integrin (Serotec); and MluC5, rabbit anti-67-kDa laminin receptor (34) were used in this study.

All chemicals used were from Sigma except for cyclosporine (Calbiochem, Nottingham, United Kingdom), staurosporine (Calbiochem), and acrylamide (BDH Laboratories, Poole, United Kingdom). All inhibitors were preincubated with the cells for 30 min before incubation with HPE, followed by coincubation with HPE during 1 h.

Immunofluorescence. Monolayers growing in transparent semipermeable tissue culture inserts (Falcon) were washed and fixed with 4% paraformaldehyde at room temperature for 30 min. Monolayers were permeabilized with 0.5% Triton X-100 and incubated in blocking solution (phosphate-buffered saline [PBS] containing 3% nonfat dry milk) followed by the primary antibody for 1 h. Cells were then washed and incubated with the appropriate fluorescein isothiocyanate-conjugated secondary antibody in blocking solution (PBS containing 0.05% Tween 20 and 3% nonfat dry milk). After incubation, the filters were washed, punched out, and mounted on glass slides.

All images were acquired with a Nikon Diaphot (Nikon Europe, Badhoevedozp, The Netherlands) inverted phase-contrast and fluorescence microscope. Processing of acquired photographic images was performed using Adobe Photoshop software (San Jose, Calif.).

Measurement of I_{sc}. Confluent monolayers of T84 cells were grown on collagen-coated permeable supports and maintained until steady-state transepithelial resistance (>1,000 Ω/cm^2) was achieved. To measure short-circuit currents (I_{sc}), transepithelial potentials, and resistance, a commercially available voltage clamp (Iowa Dual Voltage Clamps, Bioengineering, University of Iowa) interfaced with an equilibrated pair of calomel electrodes and a pair of Ag-AgCl electrodes was utilized, as described in detail elsewhere (11). Using these values and Ohm's law (voltage = current × resistance), tissue resistance and transepithelial current were calculated. Fluid resistance within the system accounts for less than 5% of total transepithelial resistance. For experimentation, HPE or control media were diluted 1:2 in Hank's balanced salt solution and exposed to the apical and basolateral epithelial surfaces. I_{sc} was monitored over 20 min, and to demonstrate that monolayers were capable of I_{sc} monolayers were exposed to forskolin (3 μM; Calbiochem) and monitored for I_{sc}. All experiments were performed in a 37°C room to ensure that epithelial monolayers, solutions, plasticware, etc., were maintained at a uniform 37°C temperature. Tissue culture supplies were obtained from Gibco Laboratories (St. Lawrence, Mass.) and Costar (Cambridge, Mass.).

LPS and protein quantification. The protein concentration in HPE (0.5 mg/ml) was determined by the Bradford method (5). Quantification of endotoxin units in HPE ($5.7 \times 10^3 \pm 0.593 \times 10^3$ endotoxin units/ml) was performed by Bio-Whittaker (Berkshire, United Kingdom) using the *Limulus* amebocyte lysate assay.

Electron microscopy. Filters were carefully cut out from their plastic supports and processed according to the method of Orzech et al. (40). Briefly, cells were fixed for 30 min at room temperature with a mixture of 2% (wt/vol) paraformaldehyde, 1% (vol/vol) glutaraldehyde dissolved in phosphate buffer (0.1 M NaH_2PO_4, 0.1 M Na_2HPO_4; pH 7.4). Postfixation was performed in a mixture of osmic acid tetroxide (1%, vol/vol) and potassium ferricyanide (1.5%, wt/vol) in 5 mM cacodylate buffer, pH 7.0, for 1 h. After washing in cacodylate buffer, sections were dehydrated in ascending grades of alcohol and treated with propylene oxide for 45 min before embedding in Epon resin at 60°C overnight. Ultrathin sections were cut with a glass knife ultramicrotome (Reichert OMU3) and stained with uranyl acetate and lead citrate. Sections were analyzed under a Hitachi-7000 transmission electron microscope.

Apoptosis detection and assessment of cell viability. The ApopTag in situ apoptosis detection kit (Intergen Company) was used according to the manufacturer's instructions. Cell viability in HPE-treated T84 monolayers was assessed by staining with fresh 50 mM ethidium bromide and 10 mM acridine orange in PBS and subsequent examination under an inverted fluorescence microscope.

Data analysis. For clarity, TER data are expressed in time course format graphics as the percentage of the control value at the beginning of each experiment. Detachment was quantified by calculating the total number of domes as a percentage of the control. This quantification method was appropriate, since within each experiment domes had a homogeneous size. All experiments were performed individually and repeated at least three separate times. Graphs and figures show data from a representative experiment except when indicated otherwise.

RESULTS

Stimulation of polarized epithelial monolayers with HPE induces the formation of domes in a laminin-dependent man-

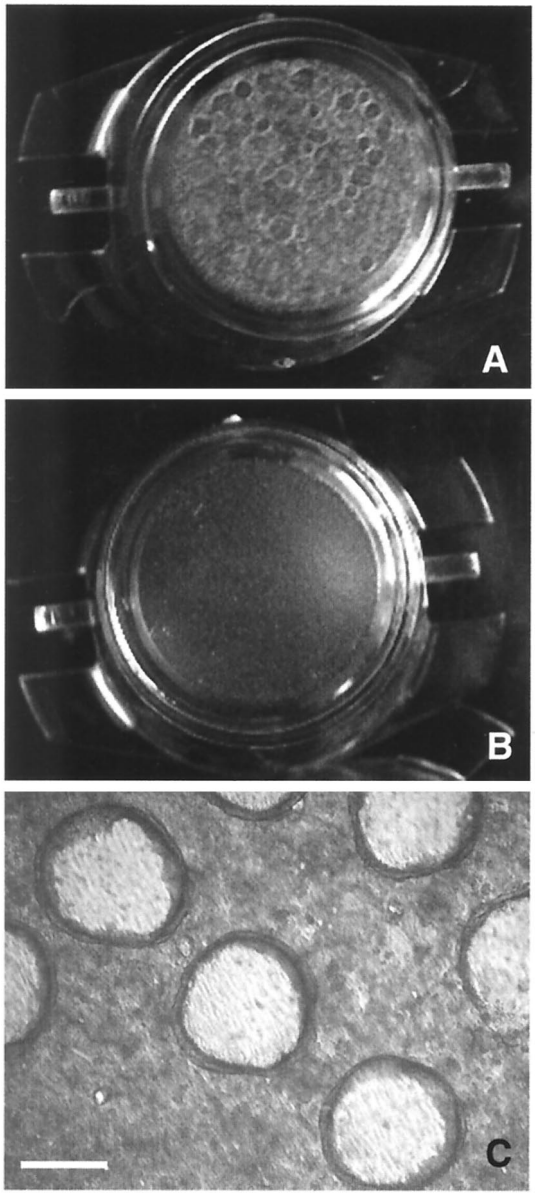

FIG. 1. HPE induce epithelial dome formation. T84 monolayers were grown in semipermeable tissue culture PET inserts and apically stimulated with HPE for 1 h at 37°C. Numerous circular structures appeared in the treated monolayers (A) but not in the controls (B). These structures could be seen with the naked eye. Images shown are from a real-time video recording (A and B) and a phase-contrast image of HPE-treated unfixed cells taken with an inverted microscope (C). Bar = 0.2 mm.

ner. To determine the response of polarized epithelia to HPE, the T84 colonic epithelial cell line growing in semipermeable tissue culture inserts was used. The apical bathing medium was substituted with HPE, and monolayers were examined in situ under a phase-contrast microscope. After 30 to 50 min of incubation at 37°C, numerous circular structures appeared evenly spread across the monolayers (Fig. 1). Phase-contrast microscopic observations indicated that each one of these structures corresponded to epithelial blisters due to cell-matrix, but not cell-cell, detachment (Fig. 2), and their formation was associated with a significant decrease in the TER (Fig. 3A). As previously shown with bacterial sonicates (55), basolateral exposure of polarized T84 monolayers to HPE did not alter TER values (data not shown), nor did it induce cell detachment (Fig. 3B). These blisters have been previously described in transporting epithelia and referred to as domes (25).

The influence of different extracellular matrix substrates on HPE-induced dome formation and TER drop was assessed by growing T84 cells on fibronectin-, collagen-, and laminin-coated inserts, as well as in polyester plastic semipermeable membranes. In all cases, apical stimulation with HPE induced a significant drop in TER (Fig. 3C). Dome formation, however, was dependent upon the biochemical composition of the extracellular matrix (Fig. 3D). A large number of domes was observed in cells growing on PET plastic and the laminin-coated insert, but domes were absent in monolayers on polyester plastic or on collagen-coated inserts. Cells grown in fibronectin-coated inserts developed domes, although to a much lesser extent than PET- or laminin-grown cells. Furthermore, preincubation of HPE with soluble laminin abolished the ability of HPE to induce dome formation (Fig. 3E). When cells were incubated with soluble laminin, washed, and then stimulated with HPE, dome formation occurred as before (Fig. 3F). This indicates that laminin binds to elements in HPE rather than to cellular receptors.

HPE-induced domes occur only in human intestinal transporting epithelia, and they are not associated with apoptosis or cell death. T84 cells cultured under the conditions defined above differentiate in vitro into polarized monolayers with two domains, apical and basolateral, which have very different membrane compositions (28). To determine if the state of differentiation of the cells influenced HPE-induced epithelial dome formation, T84 cells at different stages of maturation were analyzed. TER drop and dome formation only occurred after 13 and 15 days in culture, respectively (Fig. 4A and B), at which stage the cells are fully confluent, have reached stable TER values, and are polarized and differentiated (29). We used various epithelial cell lines to investigate cell-type-specific responses to HPE. HPE failed to induce domes in monolayers of the nontransporting epithelial cell lines AGS (gastric) and HTC116 (colonic) or in the canine renal cell line of transporting epithelial cells, MDCK. Caco-2-transporting epithelia (colonic) responded to HPE stimulation, as T84 did, by forming domes (Fig. 4C).

HPE-induced dome formation was not associated with cell death, since staining of treated monolayers with ethidium bromide-acridine orange up to 6 h after cell-matrix detachment indicated that all cells were viable (data not shown), and replacement of HPE with fresh medium for 24 h facilitated reattachment and recovery of normal TER levels (Fig. 4D). Furthermore, microscopic observation upon monolayer staining with the ApopTag in situ apoptosis detection kit confirmed that the cells were not apoptotic (data not shown).

Epithelial detachment is specifically caused by *H. pylori*. To determine strain and species specificities associated with the formation of domes, we used extracts from different strains of *H. pylori* whose phenotypes and associations with disease are known (33) as well as two gram-negative bacteria, *E. coli* and *S. marcescens* (Fig. 5A). In all cases, cells were apically stimulated with 0.5 ml of extract per cm^2 of monolayer. As shown

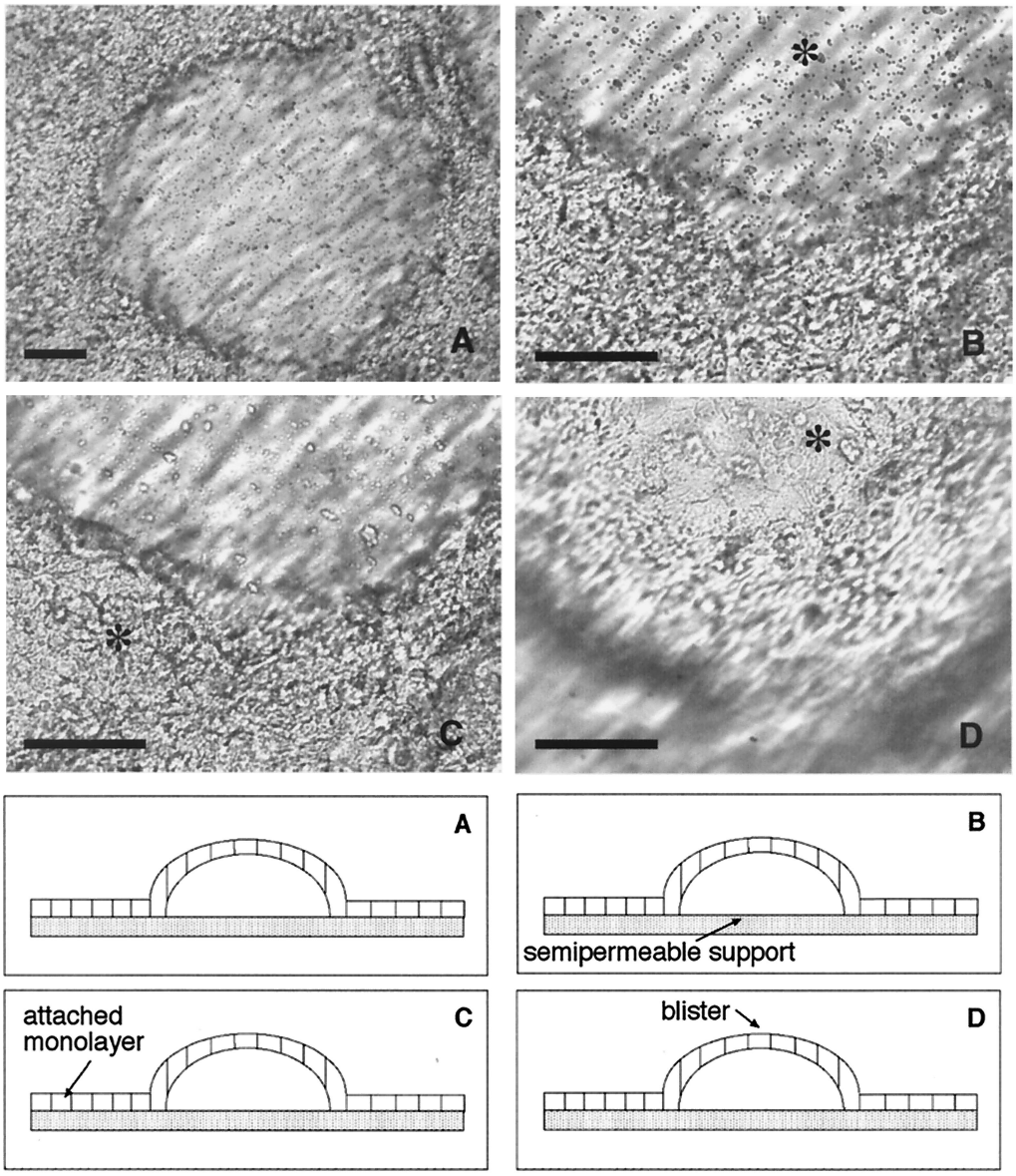

FIG. 2. Phase-contrast microscopy of epithelial-matrix, but not cell-cell, detachment in HPE-treated monolayers. (A) Magnified dome as seen with an inverted phase-contrast microscope. Domes correspond to areas in which the monolayer is detached from the substrate. (B to D) Sequence of images of the monolayer taken as it is focused from the bottom to the top of the dome. The diagrams represent a transverse section of panels A to D. Arrows in the diagrams correspond to the asterisks in the photographs. Sequential focusing shows the porous support (B), the attached monolayer above it (C), and then the detached cells at the top of the dome (D). Bar = 300 μm.

in Fig. 5B, all strains of *H. pylori* tested induced blisters independently of their cagA, vacA, or Lewis x or y phenotype, while extracts from neither *E. coli* nor *S. marcescens* induced significant detachment. Furthermore, HPE-induced dome formation was dose dependent (Fig. 5C). Since urease, vacA, and cagA are some of the major determinants in *H. pylori* pathogenesis and they can have significant effects in cell physiology (reviewed in reference 38), we further studied the capacity of HPE from isogenic mutants for these proteins to induce dome formation. We used HPE from two different vacA$^-$ isogenic mutant strains, 60190 and 84183, one CagA$^-$ isogenic mutant strain, and isogenic mutants for ureB and ureG, which are essential for urease expression (13, 15). HPE from both the wild type and mutants were able to induce dome formation (Fig. 5D).

Dome formation involves epithelial basolateral separation between neighboring cells due to cell shrinkage. Ultrastructural analysis by transmission electron microscopy showed deep morphological changes in HPE-treated monolayers compared to controls (Fig. 6A and B). In control monolayers, the cells appeared tightly joined to each other, maintaining their tight junctions and with their apical and basolateral domains well differentiated (Fig. 6A, C, and E). At the domes, the cells also maintained their polarity, with the apical microvillae and the nucleus in a basal position, but there was extensive baso-

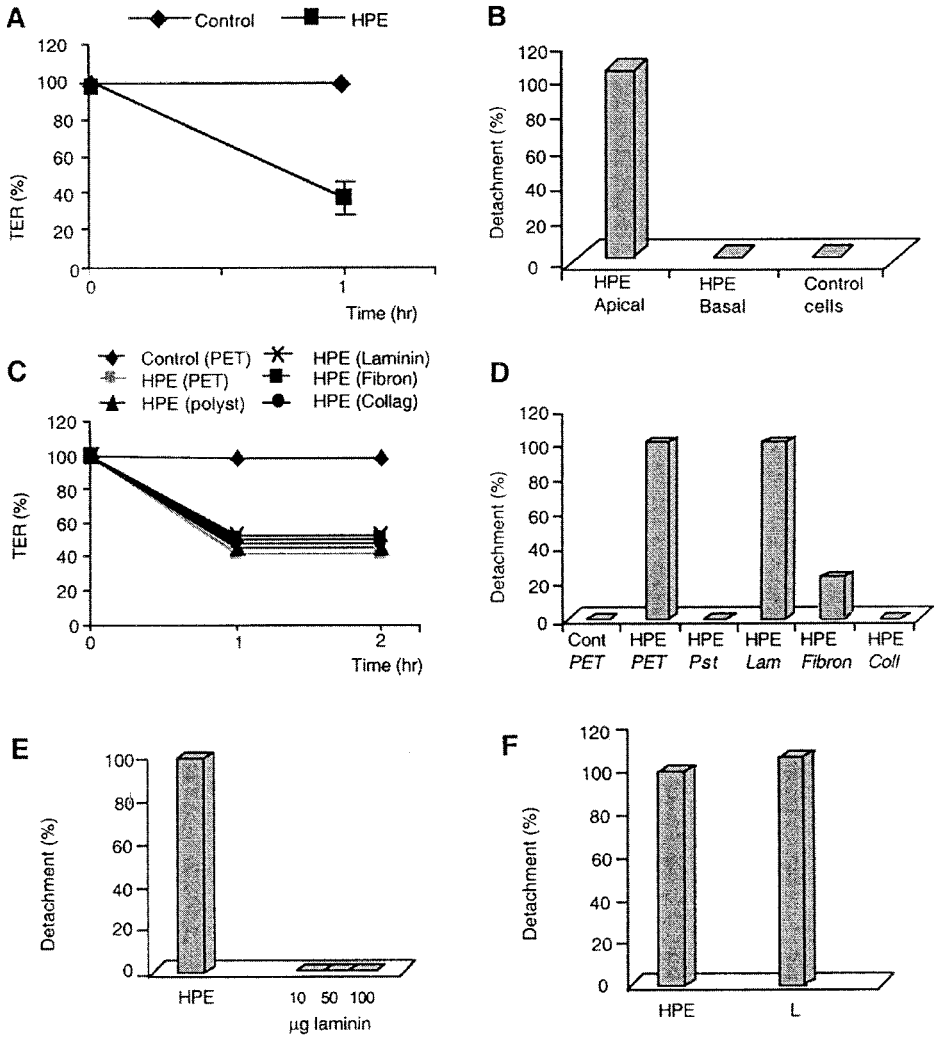

FIG. 3. Dome formation is accompanied by a decrease in TER and is inhibited by soluble laminin. Monolayers were grown in PET semipermeable inserts and stimulated with HPE for 1 h. (A and C) TER was measured with an Endhom electrode and is represented as the percentage of control values at the beginning of the experiment. (B to D) Epithelial detachment was quantified by the number of domes and is represented as a percentage of the positive control (monolayer apically treated with HPE for 1 h) of every experiment. HPE-treated monolayers had a reduced TER (A), independent of the nature of the substrate on which they were grown (PET or polyester plastic, laminin, fibronectin, or collagen) (C). However, they primarily developed domes when grown on PET or laminin (D) and only when they were apically, but not basally, stimulated with HPE (B). (E) The effect of soluble laminin in HPE-induced dome formation was subsequently assessed. HPE was preincubated for 10 min with three concentrations of soluble laminin as indicated and then used to apically stimulate the cells for comparison with untreated HPE. (F) Alternatively, monolayers were treated with 10 μg of soluble laminin (L) diluted in tissue culture medium for 30 min, then washed and incubated with HPE, and compared to monolayers only treated with HPE and without laminin preincubation (HPE).

lateral separation between neighboring cells (Fig. 6F), probably due to obvious cell shrinkage.

Influence of ENaC and Na^+/K^+ ATPase inhibition on the formation of domes. Dome formation has been associated with the occurrence of Na^+-transporting events in electrically tight epithelia (25, 61). In addition to electroneutral absorption by parallel exchange of Na^+/H^+ and Cl^-/HCO_3^-, epithelial cells possess a mechanism for electrogenic uptake of Na^+. The ENaC, which is located in the apical membrane and is potently inhibited by amiloride, is responsible for this electrogenic transport. Intracellular sodium ions are pumped out again at the basolateral side by the Na^+/K^+ ATPase, which is inhibited by ouabain (reviewed in reference 24). This pump generates the driving force for the luminal Na^+ uptake by lowering intracellular Na^+ concentration. To determine the association of HPE-induced dome formation with Na^+-transporting events, monolayers were preincubated with both inhibitors, amiloride and ouabain, for 30 min prior coincubation of the inhibitor with HPE for a further hour. Apical treatment with 0.5 mM amiloride alone induced the formation of a small number of domes even before stimulation with HPE. Addition of HPE further exacerbated the formation of domes in an amiloride dose-dependent manner (Fig. 7A). On the contrary, ouabain inhibited HPE induction of dome formation, also in an ouabain dose-dependent manner (Fig. 7B). The fact that amiloride can by itself induce the formation of domes indicates that these structures form as a consequence of intracellular Na^+ depletion, which would be driven by the Na^+/K^+ ATPase in the

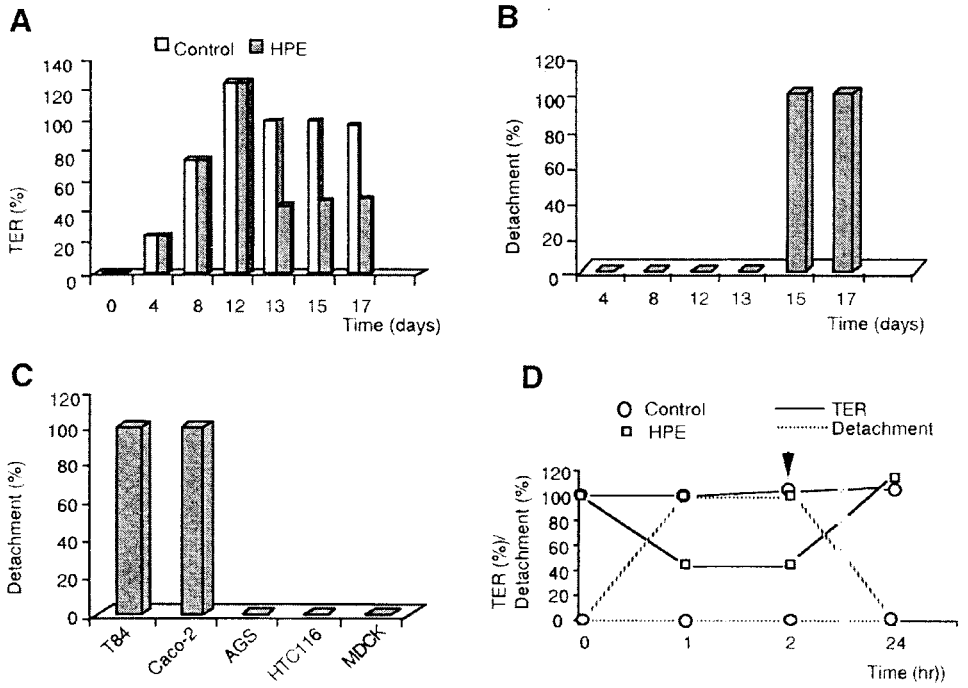

FIG. 4. Dome formation is reversible and only occurs in transporting epithelia. Cells were grown and analyzed as indicated in the legend for Fig. 3. (A and B) The effect of monolayer age on HPE-induced TER decrease and dome formation was assessed. (C) HPE-induced dome formation was also assessed in different cell lines, as indicated. (D) Reversibility of dome formation and TER decrease was assessed by replacing HPE with normal tissue culture medium (arrow) and culturing the cells overnight.

absence of Na^+ intake. Hence, HPE could be inducing intracellular Na^+ depletion, which would in turn cause cellular shrinkage, as determined by electron microscopy.

Dome formation is not accompanied by chloride secretion. Na^+ depletion could be generated by direct or indirect inactivation of ENaC or the electroneutral Na^+ channels (Na^+/H^+ exchangers, NHE2 and -3). ENaC has been shown to be negatively regulated by activation of the cystic fibrosis transmembrane conductance regulator (CFTR). After stimulation of wild-type CFTR by cAMP, amiloride-sensitive Na^+ absorption is inhibited (24, 31). Hence, we measured electrogenic Cl^- secretion upon stimulation of T84 monolayers with HPE to determine if HPE would cause intracellular sodium depletion by acting as a secretagogue. However, HPE did not induce Cl^- secretion above that of the control monolayers (Fig. 8), although both control and treated cells retained Cl^- secretion capacity as shown by stimulation with forskolin (Fig. 8).

HPE-induced dome formation is inhibited by cytoskeletal disruption, is energy dependent, and is not inhibited by blockage of protein synthesis. The cytoskeleton is composed of actin filaments, microtubules, and intermediate filaments and is vital for many cellular processes, including mechanical strength, movement, adhesion, polarity, and intracellular trafficking (58). Cytochalasin B, colchicine, taxol, and acrylamide were used to evaluate the involvement of the actin cytoskeleton, microtubule, and intermediate filament networks, respectively, in HPE-induced dome formation. All cytoskeletal disrupters inhibited HPE-induced dome formation in a concentration-dependent manner (Fig. 9A) with the exception of cytochalasin D, which was inhibitory at all concentrations tested (Fig. 9A).

Metabolic inhibition with sodium azide also prevented the formation of domes in a concentration-dependent manner (Fig. 9B), indicating that the process is energy dependent and supporting the involvement of Na^+/K^+ ATPase. The process, however, was independent of protein synthesis, as pretreatment of monolayers with cycloheximide did not have any significant effect on dome formation (Fig. 9B).

***H. pylori*-induced dome formation is inhibited by staurosporine and herbimycin A.** The ENaC has been shown to be regulated also by intracellular signaling pathways involving different kinase families in different cell types, such as protein kinase C (PKC) (3), Src (18), or SGK (21). A series of inhibitors were used to determine the involvement of general signaling pathways in *H. pylori*-induced dome formation. Monolayers were preincubated with the inhibitors for 30 min and then coincubated with HPE for a further hour. Staurosporine is a relatively nonselective kinase inhibitor which blocks many kinases to at least some degree, while herbimycin A is a potent and cell-permeable inhibitor of tyrosine kinases. Both kinase inhibitors greatly inhibited the formation of domes (Fig. 9C), while neither pertussis toxin, a trimeric G protein inhibitor, nor cycloporin, an inhibitor of phosphatase 2B, had any significant influence in HPE-induced dome formation (Fig. 9C).

HPE-induced cell-matrix detachment is associated with anomalous expression and relocation of α6 and β4 integrins and the nonintegrin monomeric 67-kDa laminin receptor (67LR) in confluent monolayers. It has been postulated that domes are areas in which an epithelium attaches weakly to the substratum (52). Since the α6 integrin subunit, coupled to β1 or β4 integrin, is the main integrin involved in mediating gastrointestinal epithelial cell-matrix attachment (reviewed in ref-

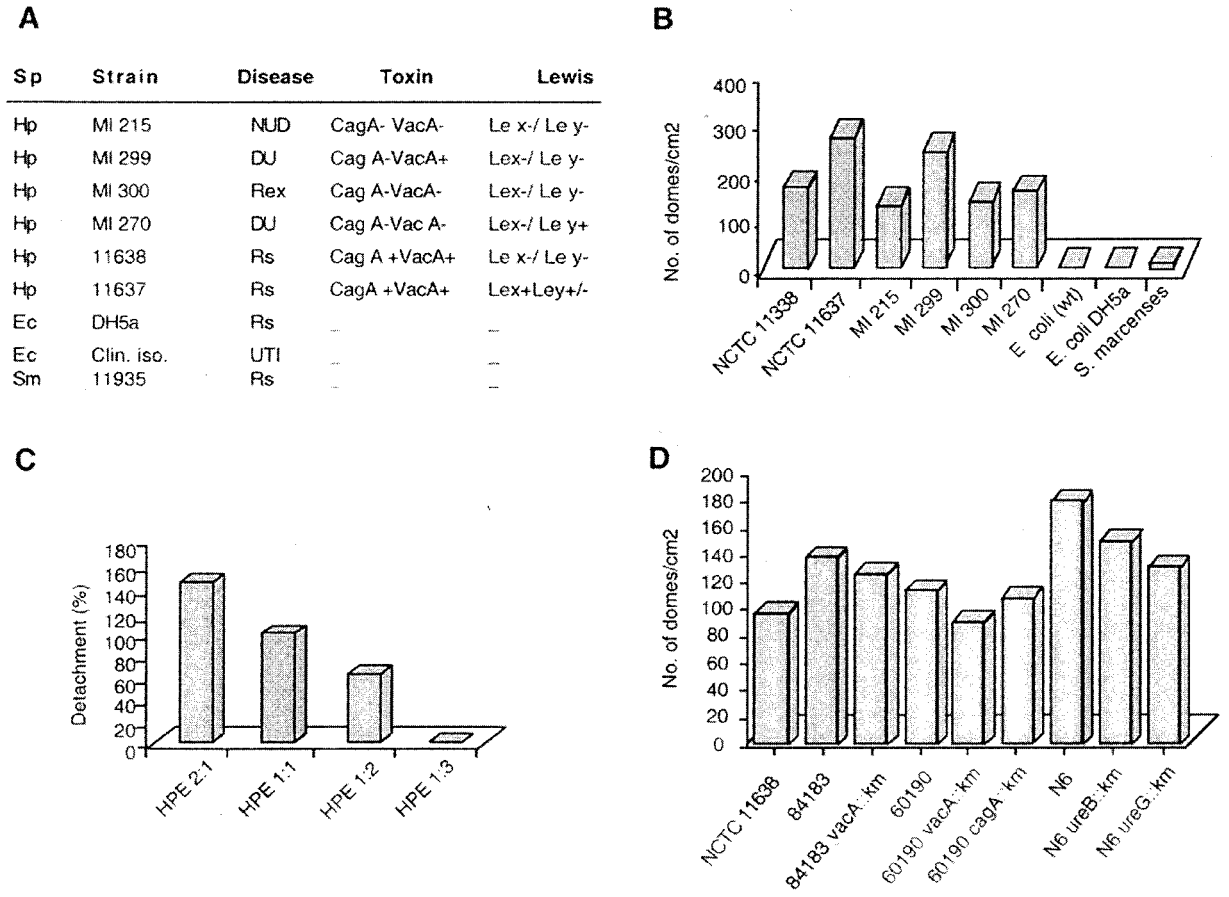

FIG. 5. HPE specifically induces dome formation in a concentration-dependent manner and is independent of the urease, VacA, CagA, and Lewis x and y phenotypes of the strains. (A) The capacity to induce domes was tested with extracts from *H. pylori* strains of defined phenotype (26). NUD, nonulcer dyspepsia; DU, duodenal ulcer; Rex, reflux esophagitis; Rs, reference strain; UTI, urinary tract infection; Le x, Lewis x; Le y, Lewis y. (B) Dome formation was assessed with extracts from *H. pylori* reference strains NCTC 11637 and 11638, as well as clinical isolates MI 215, 229, 300, and 270. Extracts from *E. coli* (wt = wild type clinical isolate; DH5α = cloning vector) and *S. marcescens* were used for comparative purposes. (C) Monolayer stimulation with serial dilutions of HPE from NCTC 11638 showed that dome formation was concentration dependent. The number of domes (detachment) is expressed as a percentage of the number of domes induced by undiluted HPE from strain NCTC 11638. (D) The specific involvement of urease, VacA, and CagA in dome formation was assessed by stimulating T84 monolayers with HPE from parental wild-type strains (84183, 60190, and N6) and the corresponding isogenic mutants for vacA, cagA, ureB, and ureG under kanamycin (km) selection. Normalization between strains (B and D) was achieved by adjusting the bacterial solution to an optical density at 600 nm of 2.9 before removing cells by centrifugation.

erence 21), we utilized immunofluorescence microscopy to visualize any changes in the expression of these integrins upon dome formation. Although the expression of all three molecules was altered in HPE-treated monolayers, the most significant changes were observed on the α6 and β4 subunits.

β1 integrin was expressed in a net-like pattern in control cells which was slightly disrupted in HPE-treated cells (Fig. 10A and B). The α6 and β4 integrins were expressed in fiber-like patches at the base of the control cells (Fig. 10C and E), which were severely disrupted upon HPE treatment. Severe loss of β4 integrin expression was observed in treated monolayers (Fig. 10D), although no intracellular granularization was observed. HPE treatment also induced significant changes in the expression of α6 integrin, which appears to redistribute toward the cell edges (Fig. 10F). Intracellular granularization was observed at the blistered area (data not shown).

Ardini et al. (1) have previously shown that the α6β4 integrin physically associates and is coregulated with the monomeric 67LR in the epidermoid carcinoma cell line A431. The 67LR was expressed in control T84 cells in a footprint-like pattern (Fig. 10G) which was mainly preserved in the treated monolayers (Fig. 10 H, panel 1). However, intracellular granularization was observed at the blisters (Fig. 10H, panel 2), where the footprint-like pattern was lost (Fig. 10H, panel 3).

Dome formation only occurred in mature monolayers grown over 15 days. To determine if integrin downregulation was a cause or a consequence of dome formation, we also assessed integrin expression by immunofluorescence in nonconfluent monolayers growing on glass coverslips for 2 days. After 1 h of stimulation with HPE, there were no significant changes in the expression of α6, β1, or β4 integrin (data not shown). This indicates that integrin downregulation occurs as a consequence of dome formation in mature monolayers.

DISCUSSION

The pathological response of epithelial cells to extraluminal insults is likely to represent the initial step in the sequence of

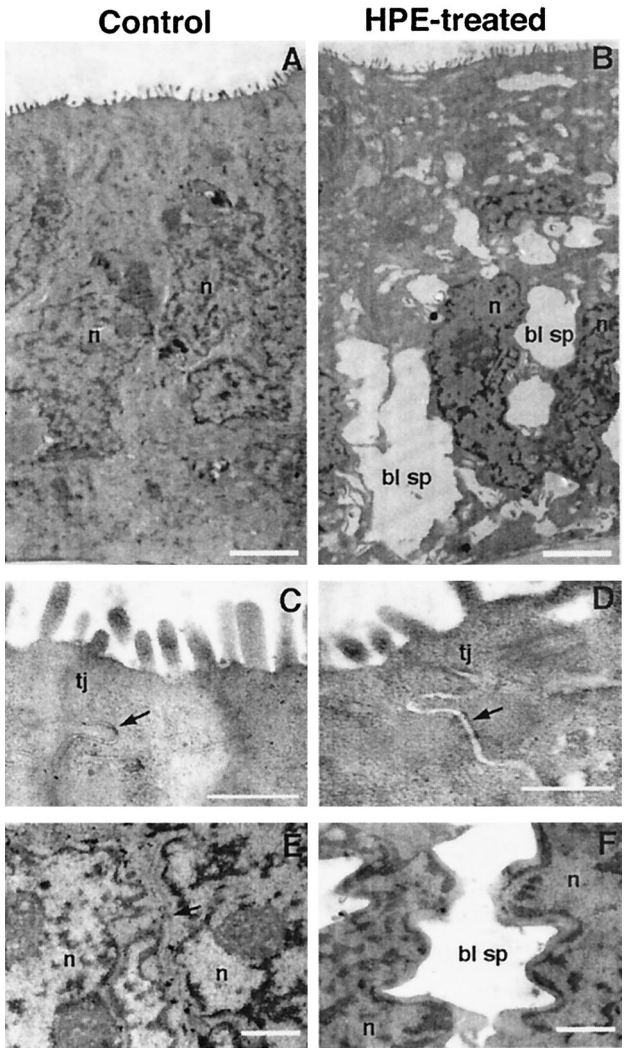

FIG. 6. Ultrastructural analysis of HPE-treated and control monolayers by transmission electron microscopy. Ultrastructural analysis by transmission electron microscopy was performed in control (A, C, and E) and treated (B, D, and F) monolayers. A full-width monolayer (A and B), apical domain (C and D), and basolateral domain (E and F) are represented. Bars: 5 μm (A and B), 0.5 μm (C and D), and 1 μm (E and F). n, nuclei; bl sp, basolateral space; tj, tight junctions.

events ultimately leading to the onset of *H. pylori*-associated pathogenesis. The epithelium is responsible for maintaining barrier function and homeostasis, limiting the indiscriminant flow of ions and macromolecules from the lumen to the lamina propria. In an in vitro model with T84 polarized epithelial monolayers, it has been previously shown (55) that sonicates and soluble extracts from the bacterium can increase epithelial permeability. More specifically, Papini et al. (42) have shown that the vacuolating toxin from *H. pylori* can increase the epithelial permeability of T84 and MDCK monolayers, independently of its vacuolating activity (44).

In this study, we showed that stimulation of T84 monolayers with *H. pylori* soluble extracts has dramatic effects on the epithelial physiological balance and integrity. Apical, but not basolateral, exposure of confluent monolayers of T84 cells to HPE induced a rapid decrease in TER as well as the formation of domes. Domes are fluid-filled blister-like areas which form due to separation of the monolayer from the substrate, while the cells remain attached to each other (47). Domes are characteristic of transporting, tight junction-forming epithelia, and they can form to a certain extent in untreated cultures after they have reached confluence in an impermeable substrate. The exact mechanism of dome formation is poorly understood. In polarized epithelial monolayers with tight junctions, domes appear to be sites of amiloride-sensitive transepithelial sodium transport (25, 61). Sugahara et al. (52) postulated that domes form due to a decreased attachment of the monolayer to the substrate. Finally, domes have also been described as a sign of differentiation in the cell culture system (26, 60).

Na^+ enters enterocytes electroneutrally, by luminal Na^+/H^+ and Cl^-/HCO_3^- exchange, or electrogenically, due to absorption via luminal ENaC. Sodium is then extruded from the cell by the Na^+/K^+ ATPase at the basolateral membrane. Coordinate activities of apical sodium channels and the basolateral sodium pump allow efficient transcellular sodium transport without affecting cell sodium concentration (24). We have shown that HPE-induced dome formation is exacerbated by amiloride, which is a potent inhibitor of ENaC. This contrasts with other reports, in which addition of amiloride has been shown to reduce the formation of domes in several cell lines (7, 12). Since domes developed spontaneously upon treatment with amiloride alone, we postulate that dome formation in this

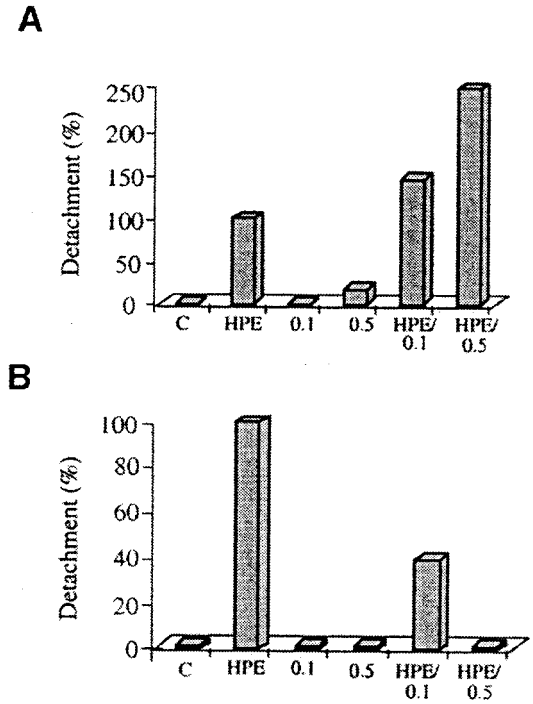

FIG. 7. Dome formation is inhibited by ouabain but exacerbated by amiloride. The effect of amiloride (A) and ouabain (B) on HPE-induced dome formation was assessed. Monolayers were pretreated with 0.1 and 0.5 mM amiloride (apical) or ouabain (basal) for 30 min prior to incubation with HPE for a further hour (HPE/0.1 and HPE/0.5) and compared to untreated controls (C), HPE-treated cells (HPE), and cells treated with the same concentrations of amiloride or ouabain alone (0.1 and 0.5).

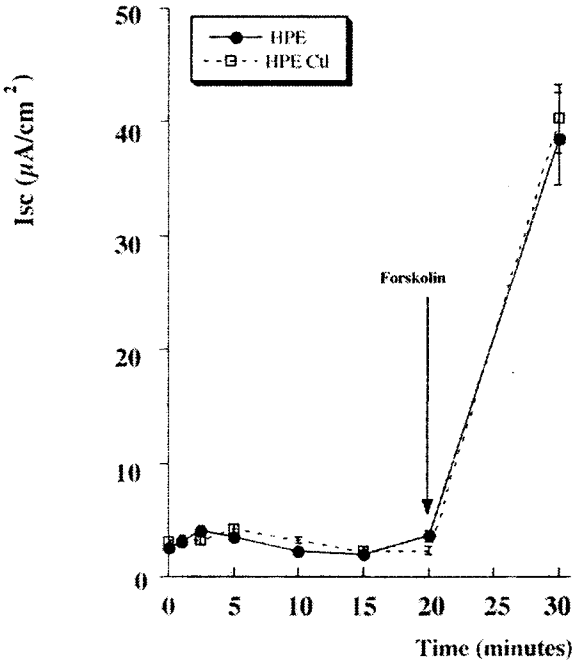

FIG. 8. Dome formation is not associated with chloride secretion. T84 intestinal epithelial monolayers were examined for induction of electrogenic Cl^- secretion by HPE. Shown here are time course curves of Cl^- secretion (measured as I_{sc}) for HPE and control. To demonstrate that cells were capable of I_{sc}, the cAMP-mediated agonist forskolin (3 μM) was added at 20 min. TER and I_{sc} were measured as indicated in Materials and Methods. Data were pooled from six to nine individual monolayers for each condition, and results are expressed as the mean peak I_{sc} ± the standard error of the mean.

cell line could be due to intracellular Na^+ depletion, driven by the basolateral Na^+/K^+ pump in the absence of an active ENaC. HPE-induced domes are accompanied by cellular shrinking, as observed by electron microscopy, which would support the association between HPE-induced domes and intracellular sodium depletion. Furthermore, the fact that the formation of HPE-induced domes is inhibited by ouabain indicates the requirement of the Na^+/K^+ ATPase and, therefore, Na^+ extravasation from the cell for the domes to occur.

We postulate that a component within HPE could be inhibiting ENaC, either directly or indirectly. ENaC inactivation by pathogens has only been shown for the influenza virus (23), which inhibits epithelial Na^+ channels in the respiratory epithelium and seems to be the only described pathogen which modulates epithelial Na^+ channels rather than Cl^- channels. ENaC regulation can be achieved at three different levels: open channel probability, channel density at the plasma membrane, and regulation of protein expression. These channels are tightly regulated by hormones such as aldosterone, vasopressin, and insulin, as well as PKA/cAMP, PKC, Ca^{2+}, and G proteins (17). The absence of Cl^- secretion upon cell stimulation with HPE indicates that PKA/cAMP is not involved in dome formation. However, the inhibition of HPE-induced dome formation by staurosporine and herbimycin A indicates the involvement of intracellular kinase pathways in this process. *H. pylori*-induced dome formation is not associated with cell death or apoptosis. Furthermore, the cells are able to reattach upon exposure to fresh medium. This indicates that in the absence of HPE the cells can restore the physiological balance of the monolayer, probably by restoring the number or activity of the appropriate channels at the plasma membrane. This would reduce the amount of accumulated fluid between the monolayer and the semipermeable substrate, facilitating cell-matrix reattachment.

The vacuolating cytotoxin from *H. pylori* is believed to be a

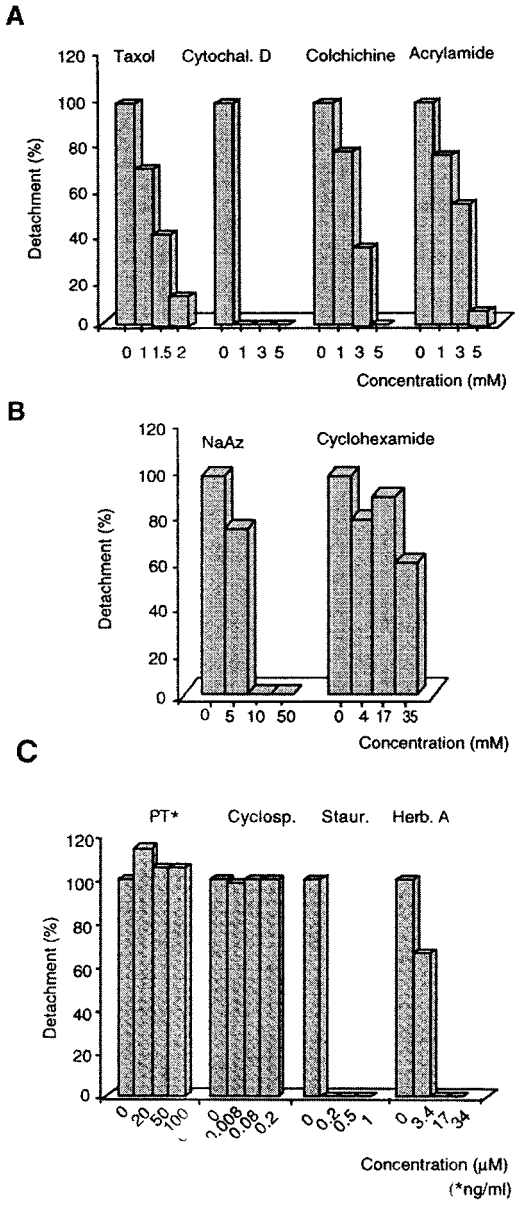

FIG. 9. Dome formation is sensitive to cytoskeletal disruption and inhibitors of phosphorylation-mediated signaling pathways. Inhibitors and disrupters were added to the cells for 30 min prior to incubation with HPE for a further hour; detachment was quantified by counting the number of domes and is represented as a percentage of the positive control treated with HPE alone within each experiment. Experiments were performed in individual inserts and repeated three separate times. The graph represents the results from a typical experiment. Cytochal. D, cytochalasin D; NaAz, sodium azide; PT, pertussis toxin; cyclosp., cyclosporine; Staur., staurosporine; Herb. A, herbimycin A.

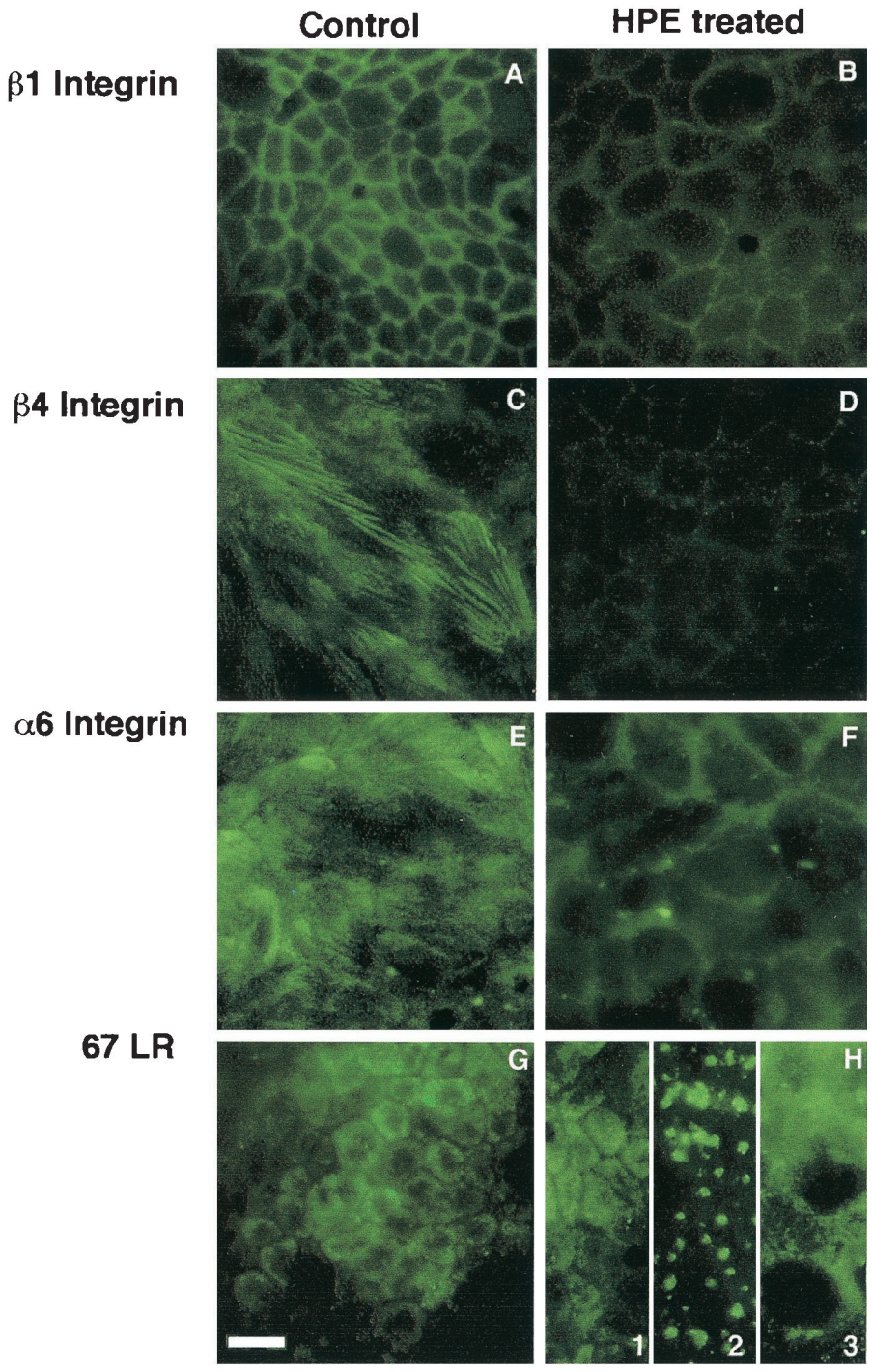

FIG. 10. Modulation of basolateral epithelial integrin distribution upon exposure to HPE. Immunofluorescence staining of control (A, C, E, and G) and HPE-treated (B, D, F, and H) monolayers for β1 integrin (A and B), α6 integrin (C and D), β4 integrin (E and F), and the 67LR (G and H). T84 polarized monolayers grown in 1-cm^2 PET tissue culture inserts were apically stimulated for 1 h with HPE. Control monolayers were maintained in medium alone. The monolayers were subsequently fixed and stained by indirect immunofluorescence with anti-β1, anti-β4, GoH3, and MluC5 antibodies and analyzed under an inverted fluorescence microscope. Bar = 30 μm.

major causative factor in the development of gastroduodenal ulcers. The toxin is secreted by the bacterium (8), forms anion-selective channels upon insertion into planar bilayers (56), and mimics CFTR-mediated chloride conductance (9). Furthermore, VacA induces a decrease in TER in T84 monolayers and an increase in paracellular permeability (42). Hence, we considered this toxin as a potential candidate which could be involved in the formation of domes. However, HPE from two different VacA mutant strains also induced dome formation, ruling out the involvement of this protein in the process.

We also considered the potential involvement of urease and CagA in dome formation, since they also have important physiological effects in epithelial cells. On the one hand, urease catalyzes the hydrolysis of urea, yielding ammonia, which produces severe cytotoxic effects within gastric epithelium (reviewed in reference 50). Furthermore, this enzyme is commonly found in association with the bacterial surface (32). On the other hand, CagA induces cytoskeletal rearrangements in epithelial cells (reviewed in reference 36), and the bacterium can induce the activation of matrix metalloproteinase-9, an enzyme capable of degrading extracellular matrix components, in a pathogenicity island-dependent way (37). Despite representing likely candidates, HPE from CagA$^-$ as well as from urease$^-$ UreB and UreG isogenic mutants were also able to induce the formation of domes, which indicates that these proteins are not involved in dome formation.

The formation of domes has been associated not only with sodium transporting events but also with decreased epithelial adherence to the substrate (52, 54). A number of observations indicate that this could be the case for HPE-induced dome formation. Firstly, dome formation was dependent upon the composition of the extracellular matrix, as it occurred mainly in those cells grown on laminin or fibronectin rather than on those grown on collagen I. Furthermore, dome formation was inhibited by HPE preincubation with soluble laminin. Since *H. pylori* LPS has been shown to bind laminin (57) and to inhibit up to 96% of the binding of laminin to the 67LR (48), the LPS component of HPE could have an important role in HPE-induced dome formation.

Long-term exposure of MDCK epithelial monolayers to retinoic acid also induces the formation of domes (54). The formation of domes in this experimental model is preceded by up to 70% inhibition of laminin biosynthesis, as well as by inhibition of synthesis of the 67LR. The 67LR has been shown to be coregulated and to associate physically with α6β4 integrin in A431 cells, where it acts as an auxiliary molecule involved in regulating or stabilizing the interaction of laminin with the integrin (1). The integrin α6β4 is the principal agent for accomplishing integration of the cytoskeleton with laminin in the extracellular matrix (51), and changes in its expression or ligand affinity lead to extensive blistering or exfoliation (45). HPE-induced dome formation is associated with dramatic changes in the pattern of expression of α6, β4, and β1 integrins, as well as the 67LR. Strikingly, β4 integrin expression was completely lost in confluent monolayers upon exposure to HPE, which indicates that dome formation associates with decreased epithelial adherence to the substrate. In nonconfluent, undifferentiated monolayers of T84 cells, short-term treatment with HPE did not lead to changes in expression of these integrins, which indicates that integrin downregulation occurs as a consequence of dome formation, and not vice versa.

H. pylori-induced epithelial disengagement from the lamina propria could contribute to the development of gastric or duodenal ulceration in conjunction with other factors which are well known to be involved in this process, such as alterations of the gastrin-somatostatin balance and a subsequent increase in acid secretion (19, 27), or the underlying inflammatory response (30). The release of reactive oxygen intermediaries from transmigrating neutrophils at the epithelium (41, 49) as well as alterations of the proliferative-apoptotic balance of epithelial cells (38) are also factors which have been postulated to contribute to epithelial denudation and therefore could facilitate the ulceration process.

In summary, these data indicate that intestinal epithelial cells develop a pathophysiological response upon treatment with soluble components from *H. pylori* which involves alteration of barrier function, changes in the physiological balance of electrolyte transport, and diminished adherence to the extracellular matrix. These effects, which are only apparent when using polarized transporting gastrointestinal epithelia as a model, represent a novel perspective for the understanding of *H. pylori*-associated pathogenesis and highlight the importance of the physiological consequences of the bacterium-epithelium interaction.

ACKNOWLEDGMENTS

We thank Y. Volkov, D. Ni Eídhin, and the Electron Microscopy Unit at Trinity College for technical assistance and B. Kiely, H. Roche, S. Beesley, and C. Herra for their kind gifts of cell lines or bacterial strains. We also thank Sean P. Colgan for carrying out the chloride secretion studies, John Atherton for the VacA mutants, Richard Peek for the CagA mutants, and Arnoud van Vliet for the UreB and UreG mutants.

This work was supported by a TMR Marie Curie fellowship to A. M. Terrés and subsequently by Enterprise Ireland.

REFERENCES

1. **Ardini, E., E. Tagliabue, A. Magnifico, S. Buto, V. Castronovo, M. I. Colhaghi, and S. Menard.** 1997. Co-regulation and physical association of the 67-kDa monomeric laminin receptor and the α6β4 integrin. J. Biol. Chem. **272:**2342–2345.
2. **Ashorn, M., F. Cantet, K. Mayo, and F. Megraud.** 2000. Cytoskeletal rearrangements induced by *Helicobacter pylori* strains in epithelial cell culture: possible role of the cytotoxin. Dig. Dis. Sci. **45:**1774–1780.
3. **Awayda, M.** 2000. Specific and nonspecific effects of protein kinase C on the epithelial Na^+ channel. J. Gen. Physiol. **115:**559–570.
4. **Barrett, K.** 2000. New insights into the pathogenesis of intestinal dysfunction: secretory diarrhea and cystic fibrosis. World J. Gastroenterol. **6:**470–474.
5. **Bradford, M. M.** 1976. A rapid and sensitive method for the quantitation of microgram quantities of protein utilizing the principle of protein-dye binding. Anal. Biochem. **72:**248–254.
6. **Braghimov, A., and J. Pappo.** 2000. The immune response against *Helicobacter pylori*—a direct linkage to the development of gastroduodenal disease. Microbes Infect. **2:**1073–1077.
7. **Brouard, M., M. Casado, S. Djelidi, Y. Barrandon, and N. Farman.** 1999. Epithelial sodium channel in human epidermal keratinocytes: expression of its subunits and relation to sodium transport and differentiation. J. Cell Sci. **112:**3343–3352.
8. **Bumman, D., S. Aksu, M. Wendland, K. Janek, U. Zimny-Arndt, N. Sabarth, T. Meyer, and P. Jungblut.** 2002. Proteome analysis of secreted proteins of the gastric pathogen *Helicobacter pylori*. Infect. Immun. **70:**3396–3403.
9. **Campello, S., F. Tombola, G. Cabrini, and M. Zoratti.** 2002. The vacuolating toxin of *Helicobacter pylori* mimics the CFTR-mediated chloride conductance. FEBS Lett. **532:**237–240.
10. **Cover, T., M. Tummuru, P. Cao, S. Thompson, and M. Blaser.** 1994. Divergence of genetic sequences for the vacuolating cytotoxin among *Helicobacter pylori* strains. J. Biol. Chem. **269:**10566–10573.
11. **Dharmsathaphorn, K., and J. Madara.** 1990. Established intestinal cell lines as model systems for electrolyte transport studies. Methods Enzymol. **192:** 354–389.
12. **Dreher, D., and T. Rochat.** 1992. Hyperoxia induces alkalinization and dome formation in MDCK epithelial cells. Am. J. Physiol. **262:**C358–C364.
13. **Eaton, K., and S. Krakowka.** 1994. Effect of gastric pH on urease-dependent colonization of gnotobiotic piglets by *Helicobacter pylori*. Infect. Immun. **62:**3604–3607.
14. **Fan, X., H. Gunasena, Z. Cheng, R. Espejo, S. E. Crowe, P. B. Ernst, and V. E. Reyes.** 2000. *Helicobacter pylori* urease binds to class II HHC on gastric epithelial cells and induces their apoptosis. J. Immunol. **15:**1918–1924.
15. **Ferrero, R., V. Cussac, P. Courcoux, and A. Labigne.** 1992. Construction of isogenic urease-negative mutants of *Helicobacter pylori* by allelic exchange. J. Bacteriol. **174:**4212–4217.
16. **Fontao, L., J. Stutzmann, P. Gendry, and J. F. Launay.** 1999. Regulation of the type II hemidesmosolam plaque assembly in intestinal epithelial cells. Exp. Cell Res. **250:**298–312.

17. **Garty, H., and L. Palmer.** 1997. Epithelial sodium channels: function, structure and regulation. Physiol. Rev. **77:**359–396.
18. **Gilmore, E., M. Stutts, and S. Milgram.** 2001. SRC family kinases mediate epithelial Na^+ channel inhibition by endothelin. J. Biol. Chem. **276:**42610–42617.
19. **Graham, D. Y., A. Opekun, G. M. Lew, P. D. Klein, and J. H. Walsh.** 1991. *Helicobacter pylori*-associated exaggerated gastrin release in duodenal ulcer patients. The effect of bombesin infusion and urea ingestion. Gastroenterology **100:**1571–1575.
20. **Kalia, N., K. Bardhan, J. Atherton, and N. Brown.** 2002. Toxigenic *Helicobacter pylori* induces changes in the gastric mucosal microcirculation of rats. Gut **51:**641–647.
21. **Kamynina, E., and O. Staub.** 2002. Concerted action of ENaC, Nedd4–2 and Sgk 1 in transepithelial Na^+ transport. Am. J. Physiol. Renal Physiol. **283:** F377–F387.
22. **Kim, H., J. W. Lim, and K. H. Kim.** 2001. *Helicobacter pylori*-induced expression of interleukin-8 and cyclooxygenase-2 in AGS gastric epithelial cells: mediation by nuclear factor-κB. Scand. J. Gastroenterol. **36:**706–716.
23. **Kunzelmann, K., A. Beesley, N. King, G. Karupiah, J. Young, and D. Cook.** 2000. Influenza virus inhibits amiloride-sensitive Na^+ channels in respiratory epithelia. Proc. Natl. Acad. Sci. USA **97:**10282–10287.
24. **Kunzelmann, K., and M. Mall.** 2001. Electrolyte transport in the mammalian colon: mechanisms and implications for disease. Physiol. Rev. **82:**245–289.
25. **Lever, J.** 1979. Inducers of mammalian cell differentiation stimulate dome formation in a differentiated kidney epithelial cell line (MDCK). Proc. Natl. Acad. Sci. USA **76:**1323–1327.
26. **Lever, J.** 1979. Regulation of dome formation in differentiated epithelial cell cultures. J. Supramol. Struct. **12:**259–272.
27. **Levi, S., K. Beardshall, G. Haddad, R. Playford, P. Ghosh, and J. Calam.** 1989. Campylobacter pylori and duodenal ulcer disease: the somatostatin link? Lancet **i:**1167–1168.
28. **Madara, J., J. Stafford, K. Dharmsthaphorn, and S. Carlson.** 1987. Structural analysis of a human intestinal epithelial cell line. Gastroenterology **92:**1133–1145.
29. **Madara, J. L., and K. Dharmsathaphorn.** 1985. Occludin junction structure-function relationships in a cultured epithelial monolayer. J. Cell Biol. **101:** 2124–2133.
30. **Madsen, J. E., K. Vetvik, and S. Aase.** 1991. *Helicobacter pylori* and chronic active inflammation of the duodenum and stomach in duodenal ulcer patients treated with ranitidine, misoprostol or an acid-neutralising agent. Scand. J. Gastroenterol. **26:**465–470.
31. **Mall, M., M. Bleich, R. Greger, R. Schreiber, and K. Kunzelmann.** 1998. The amiloride-inhibitable Na^+ conductance is reduced by the cystic fibrosis transmembrane conductance regulator in normal but not in cystic fibrosis airways. J. Clin. Investig. **102:**15–21.
32. **Marcus, E., and D. Scott.** 2001. Cell lysis is responsible for the appearance of extracellular urease in *Helicobacter pylori*. Helicobacter **6:**93–99.
33. **Marshall, D., S. Hynes, D. Coleman, C. O'Morain, C. Smyth, and C. Moran.** 1999. Lack of relationship between Lewis antigen expression and cagA, CagA, vacA and VacA status of Irish *Helicobacter pylori* isolates. FEMS Immunol. Med. Microbiol. **24:**79–90.
34. **Martignone, S., R. Pellegrini, E. Villa, N. Tandon, A. Mastroianni, E. Tagliabue, S. Menard, and M. Colnaghi.** 1992. Characterization of two monoclonal antibodies directed against the 67 kD high affinity laminin receptor and application for the study of breast carcinoma progression. Clin. Exp. Metastasis **10:**379–386.
35. **Mitic, L. L., C. M. Van-Itallie, and J. M. Anderson.** 2000. Molecular physiology and pathophysiology of the tight junctions. I. Tight junction structure and function: lessons from mutant animals and proteins. Am. J. Physiol. Gastrointest. Liver Physiol. **279:**G250–G254.
36. **Montecucco, C., and R. Rappuoli.** 2001. Living dangerously: how *Helicobacter pylori* survives in the human stomach. Nat. Rev. Mol. Cell. Biol. **2:**457–466.
37. **Mori, N., H. Sato, T. Hayashibara, M. Senba, R. Geleziunas, A. Wada, T. Hirayama, and N. Yamamoto.** 2003. *Helicobacter pylori* induces matrix metalloproteinase-9 through activation of nuclear factor κB. Gastroenterology **124:**983–992.
38. **Moss, S., J. Calam, B. Agarwal, S. Wang, and P. Holt.** 1996. Induction of gastric epithelial apoptosis by *Helicobacter pylori*. Gut **38:**498–501.
39. **Münzenmaier, A., C. Lange, E. Glocker, A. Covacci, A. Moran, S. Bereswill, P. A. Baeuerle, M. Kistg, and H. L. Pahl.** 1997. A secreted/shed product of *Helicobacter pylori* activates transcription factor nuclear factor-κB. J. Immunol. **159:**6140–6147.
40. **Orzech, E., S. Cohen, A. Weiss, and B. Aroeti.** 2000. Interaction between the exocytic and endocytic pathways in polarized Madin-Darby canine kidney cells. J. Biol. Chem. **275:**15207–15219.
41. **Papa, A., S. Danese, A. Sgambato, R. Ardito, G. Zannotni, A. Rinalli, F. Vecchio, N. Gentiloni-Silveri, A. Cittadini, G. Gasbarrini, and A. Gasbarrini.** 2002. Role of *Helicobacter pylori* $CagA^+$ infection in determining oxidative DNA damage in gastric mucosa. Scand. J. Gastroenterol. **37:**409–413.
42. **Papini, E., B. Satin, N. Norals, M. Bernard, J. L. Telford, R. Rappuoli, and C. Montecucco.** 1998. Selective increase of the permeability of polarized epithelial cell monolayers by *Helicobacter pylori* vacuolating toxin. J. Clin. Investig. **102:**813–820.
43. **Peek, R., H. Wirth, S. Moss, M. Yang, A. Abdalla, K. Tham, T. Zhang, L. Tang, I. Modlin, and M. Blaser.** 2000. *Helicobacter pylori* alters gastric epithelial cell cycle events and gastrin secretion in Mongolian gerbils. Gastroenterology **118:**48–59.
44. **Pelicic, V., J. Reyrat, L. Sartori, C. Pagliaccia, R. Rappuoli, J. Telford, C. Montecucco, and E. Papini.** 1999. *Helicobacter pylori* VacA cytotoxin associated with the bacteria increases epithelial permeability independently of its vacuolating activity. Microbiology **145:**2043–2050.
45. **Rizzi, L., L. Gagnoux-Palacios, M. Pinola, S. Belli, G. Meneguzzi, M. D'Alessio, and G. Zambruno.** 1997. A homozygous mutation in the integrin alpha 6 gene in junctional epidermolysis bullosa with pyloric atresia. J. Clin. Investig. **15:**2826–2831.
46. **Rodriguez-Boulan, E., and C. Zurzolo.** 1993. Polarity signals in epithelial cells. J. Cell Sci. Suppl. **17:**9–12.
47. **Rotoli, B., G. Orlandini, R. Gatti, V. DAll'Asta, G. Gazzola, and O. Bussolati.** 2002. Employment of confocal microscopy for the dynamic visualization of domes in intact epithelial cell cultures. Cells Tissues Organs **170:**237–245.
48. **Slomiany, B., J. Piotrowski, S. Sengupta, and A. Slomiany.** 1991. Inhibition of gastric mucosal laminin receptor by *Helicobacter pylori* lipopolysaccharide. Biochem. Biophys. Res. Commun. **29:**963–970.
49. **Smoot, D., T. Elliott, H. Verspaget, D. Jones, C. Allen, K. Vernon, T. Bremner, L. Kidd, K. Kim, J. Groupman, and H. Ashktorab.** 2000. Influence of *Helicobacter pylori* on reactive oxygen-induced gastric epithelial cell injury. Carcinogenesis **21:**2091–2095.
50. **Stingl, K., K. Altendorf, and E. Bakker.** 2002. Acid survival of *Helicobacter pylori*: how does urease activity trigger cytoplasmic pH homeostasis? Trends Microbiol. **10:**70–74.
51. **Stutzmann, J., A. Bellissent-Waydelich, L. Fontao, J. F. Launay, and P. Simon-Assmann.** 2000. Adhesion complexes implicated in intestinal epithelial cell-matrix interactions. Microsc. Res. Tech. **51:**179–190.
52. **Sugahara, K., J. Caldwell, and R. Mason.** 1984. Electrical currents flow out of domes formed by cultured epithelial cells. J. Cell Biol. **99:**1541–1544.
53. **Taub, M.** 1989. Retinoic acid modulates dome formation by MDCK cells in defined medium. J. Cell. Physiol. **141:**24–32.
54. **Taub, M.** 1991. Retinoic acid inhibits basement membrane protein biosynthesis while stimulating dome formation by Madin Darby canine kidney cells in hormonally defined serum-free medium. J. Cell. Physiol. **148:**211–219.
55. **Terrés, A. M., J. M. Pajares, A. M. Hopkins, A. Murphy, A. Moran, A. W. Baird, and D. Kelleher.** 1998. *Helicobacter pylori* disrupts epithelial barrier function in a process inhibited by protein kinase C activators. Infect. Immun. **66:**2943–2950.
56. **Tombola, F., S. Carlesso, I. Szabo, M. de-Bernard, J. Reyrat, J. Telford, R. Rappuoli, C. Montecucco, E. Papini, and M. Zoratti.** 1999. *Helicobacter pylori* vacuolating toxin forms anion-selective channels in planar lipid bilayers: possible implications for the mechanism of cellular vacuolation. Biophys. J. **76:**1401–1409.
57. **Valkonen, K., T. Wadstrom, and A. Moran.** 1994. Interaction of lipopolysaccharides of *Helicobacter pylori* with basement membrane protein laminin. Infect. Immun. **62:**3640–3648.
58. **Yang, Y., C. Bauer, G. Strasser, R. Wollman, J. P. Julien, and E. Fuchs.** 1999. Integrators of the cytoskeleton that stabilize microtubules. Cell **98:**229–238.
59. **Yap, A. S., W. M. Brieher, and B. M. Gumbiner.** 1997. Molecular and functional analysis of cadherin-based adherens junctions. Annu. Rev. Cell Dev. Biol. **13:**119–146.
60. **Zucchi, I., L. Bini, D. Albani, R. Valaperta, S. Liberatori, R. Raggiaschi, C. Montagna, L. Susani, O. Barbieri, V. Pallini, P. Vezzoni, and R. Dulbecco.** 2002. Dome formation in cell cultures as expression of an early stage of lactogenic differentiation of the mammary gland. Proc. Natl. Acad. Sci. USA **25:**8660–8665.
61. **Zucchi, I., C. Montagna, L. Susani, R. Montesano, M. Affer, S. Zanotti, E. Redolfi, P. Vezzoni, and R. Dulbecco.** 1999. Genetic dissection of dome formation in a mammary cell line: identification of two genes with opposing action. Proc. Natl. Acad. Sci. USA **23:**13766–13770.

Editor: F. C. Fang